ISSN: 2231-3656

International Journal of Pharmacy and Industrial Research (IJPIR)

IJPIR |Vol. 16 | Issue 3 | July–Sep2026

www.ijpir.com

DOI: https://doi.org/10.61096/ijpir.v16.iss3.2026.692-712

Controlled Release of Cyclosporine via In-Situ Phase Transformation in A Non-Ionic Microemulsion

Hardi Vasvaria[1]*, Sonam Gandhi[2], Bhavin Prajapati[3]

[1,3]Assistant Professor, Vidhyadeep Institute of Pharmacy, Vidhyadeep University, Anita, kim, highway, Olpad, Gujarat 394110, India,
[2]Assistant Professor, S. S. Agrawal Institute of Pharmacy, Navsari, Gujarat, India.

***Corresponding Author: Hardi Vasvaria**
Email: hardivasvaria@gmail.com

Published on: 19.07.2026
Published by: Futuristic Publications

Abstract: This study reports structural characterization of a liquid crystalline (LC) phase, formed through water driven transition in a nonionic microemulsion (ME). ME was formulated with α-tocopheryl polyethylene glycol succinate (TPGS)-Span 80 (3:1) as surfactant mixture and Captex 300 as oil phase. LC structures were characterized by polarized light microscopy and differential scanning calorimetry. Transition occurred with 19-23% water addition and it was accompanied with; (a) change of isotropic ME to birefringent LC phase, and (b) improvement in the mechanical properties. However, the transition downshifted to 9.8% water level when the oil phase was loaded with 50 mg/ml cyclosporine. LC structures remained stable at physiological temperature until 72 h and offered controlled release of cyclosporine under artificial sink conditions. We suggest that in situ development of LC phase can be explored to clear long-residing intra-muscular depots capable of discharging the payload at a controlled rate.

Keywords: microemulsion, in situ transformation, cyclosporine, liquid crystalline, controlled release, non-ionic surfactant.

1. INTRODUCTION

Cyclosporine is a cyclic undecapeptide and a potent immunosuppressive agent widely employed in the management of autoimmune disorders, including rheumatoid arthritis, and in the prevention of organ transplant rejection. Despite its remarkable therapeutic efficacy, the clinical application of cyclosporine is limited by its poor aqueous solubility, low and variable oral bioavailability, extensive first-pass metabolism, and significant fluctuations in plasma drug concentration. These drawbacks often necessitate frequent administration and may lead to dose-related adverse effects, thereby reducing patient compliance.

Rheumatoid arthritis (RA) is a chronic, progressive autoimmune inflammatory disease characterized by persistent synovial inflammation, cartilage degradation, and irreversible joint destruction. Conventional pharmacotherapy, including non-steroidal anti-inflammatory drugs (NSAIDs), corticosteroids, and disease-modifying antirheumatic drugs (DMARDs), provides symptomatic relief but is often associated with systemic toxicity and limited long-term effectiveness. Cyclosporine has demonstrated significant immunomodulatory activity in RA by suppressing T-lymphocyte activation and inhibiting cytokine production; however, its pharmaceutical limitations restrict its therapeutic potential.

Microemulsions are thermodynamically stable, transparent, isotropic dispersions composed of oil, water, surfactant, and frequently a co-surfactant. Owing to their nanometric droplet size and excellent solubilization capacity, they have emerged as promising carriers for lipophilic drugs. Non-ionic micro emulsion systems are particularly attractive because of their superior biocompatibility, lower toxicity, and enhanced formulation stability compared with ionic systems.

A unique advantage of these systems is their ability to undergo in-situ phase transformation when exposed to an aqueous biological environment. Upon contact with gastrointestinal fluids, the low-viscosity micro emulsion can spontaneously transform into highly organized liquid crystalline mesophases. These structures create a diffusion barrier that slows drug release, thereby providing sustained delivery and improving therapeutic performance.

Liquid crystalline systems have attracted considerable attention in advanced drug delivery because of their ability to accommodate both hydrophilic and lipophilic drugs, maintain structural stability, and prolong drug release. The in-situ generated liquid crystalline matrix can function as a drug reservoir, minimizing rapid drug diffusion and reducing fluctuations in systemic drug levels.

Therefore, the development of a non-ionic micro emulsion capable of in-situ phase transformation represents a promising strategy for the controlled delivery of cyclosporine. Such a system may improve drug solubility, enhance bioavailability, provide sustained release, reduce dosing frequency, and minimize dose-related toxicity, ultimately leading to improved therapeutic outcomes in the management of rheumatoid arthritis.

The present study was therefore undertaken to develop and evaluate a non-ionic micro emulsion-based in-situ phase transforming system for the controlled release of cyclosporine and to investigate its potential as an effective drug delivery platform for long-term therapy.

2. AIM AND OBJECTIVES

2.1 Aim of the Study

The present study aims to develop and evaluate a **non-ionic micro emulsion-based drug delivery system capable of undergoing in-situ phase transformation into a lipotropic liquid crystalline structure for the controlled release of cyclosporine.** The proposed system is intended to create a stable depot following aqueous dilution, thereby prolonging drug release, enhancing drug solubility, and improving the therapeutic performance of cyclosporine.

2.2 Objectives of the Study

To accomplish the above aim, the following specific objectives were established:

1. To formulate a non-ionic micro emulsion of cyclosporine using suitable oils, surfactants, and co-surfactants.
2. To construct pseudo-ternary phase diagrams for the selection and optimization of the micro emulsion composition.
3. To optimize the micro emulsion formulation with the ability to undergo **in-situ phase transformation into a lipotropic liquid crystalline system** upon aqueous dilution.
4. To characterize the developed micro emulsion and the resulting liquid crystalline system using appropriate analytical techniques.
5. To evaluate the physicochemical properties of the developed system by:
    - Dynamic Light Scattering (DLS)
    - Differential Scanning Calorimetry (DSC)
    - Polarized Optical Microscopy (POM)
    - Rheological studies
    - Texture Profile Analysis (TPA)
    - To investigate the in-vitro release profile of cyclosporine from the in-situ phase transforming non-ionic micro emulsion.
    - To assess the capability of the liquid crystalline system to provide sustained and controlled drug release.
6. To perform stability studies of the optimized formulation under appropriate storage conditions to ensure its physicochemical stability and performance.

3. MATERIALS AND METHODS

3.1 Materials

Cyclosporine was used as the model drug for the development of the controlled release formulation. Tocopherol polyethylene glycol succinate (TPGS) was selected as the non-ionic surfactant, Span 80 as the co-surfactant, and caprylic/capric triglyceride (Captex® 300) as the oil phase. Sterile purified water was used as the aqueous phase. All chemicals and solvents employed in the study were of analytical or HPLC grade and were used without further purification.

Table 1: Materials used in the study

Sr. No.	Material	Function
1	Cyclosporine	Active pharmaceutical ingredient
2	TPGS (Tocopheryl polyethylene glycol succinate)	Surfactant
3	Span 80	Co-surfactant
4	Caprylic/Capric Triglyceride (Captex® 300)	Oil phase
5	Sterile Purified Water	Aqueous phase

3.2 Instruments

The formulation and characterization studies were carried out using standard analytical instruments. Differential scanning calorimetry (DSC) was performed using a Mettler STARe SW 9.30 instrument. High-performance liquid chromatography (HPLC) analysis was conducted using a Shimadzu LC-2010C HT system. Fourier transform infrared (FTIR) spectroscopy was carried out using a Shimadzu 8400S spectrophotometer. Morphological analysis was performed using a JSM-5610 scanning electron microscope. A polarized optical microscope (Olympus) was used for the identification of liquid crystalline structures. Other laboratory equipment included a magnetic stirrer, sonicator, and digital analytical balance.

Table 2: Instruments used in the study

Sr. No.	Instrument	Manufacturer
1	Differential Scanning Calorimeter (DSC)	Mettler STARe SW 9.30
2	High Performance Liquid Chromatography (HPLC)	Shimadzu LC-2010C HT
3	FTIR Spectrophotometer	Shimadzu 8400S
4	Magnetic Stirrer	Remi
5	Scanning Electron Microscope (SEM)	JSM-5610
6	Sonicator	Shimadzu
7	Digital Analytical Balance	Sartorius
8	Polarized Optical Microscope	Olympus

3.3 Drug and Excipient Selection

Cyclosporine was selected because of its poor aqueous solubility, low oral bioavailability, and short biological half-life, making it a suitable candidate for controlled release delivery. TPGS was employed as a non-ionic surfactant due to its excellent emulsifying ability and biocompatibility. Span 80 was incorporated as a co-surfactant to improve interfacial flexibility and facilitate micro emulsion formation. Caprylic/capric triglyceride (Captex® 300) was used as the oil phase because of its high solubilisation capacity for lipophilic drugs.

3.4 Preparation and Optimization of Non-Ionic Microemulsion

The non-ionic micro emulsion system was designed by selecting appropriate ratios of oil, surfactant, and co-surfactant. Pseudo-ternary phase diagrams were constructed using the aqueous titration method to identify the micro emulsion region and optimize the formulation composition.

3.5 In-situ Phase Transformation Study

The optimized micro emulsion formulation was diluted with the aqueous phase to induce in-situ transformation into a lyotropic liquid crystalline system. The phase behavior and structural transition were observed and characterized.

3.6 Characterization of the Formulation

The developed formulation was evaluated for:

- Particle size and polydispersity index by Dynamic Light Scattering (DLS).
- Thermal behaviour by Differential Scanning Calorimetry (DSC).
- Liquid crystalline structure by Polarized Optical Microscopy (POM).
- Rheological properties.
- Texture profile analysis.
- In-vitro drug release behaviour.

3.7 Stability Studies

The optimized formulation was subjected to stability studies under suitable storage conditions, and changes in physicochemical properties and drug release characteristics were monitored over the study period.

3.8 Methodology

3.8.1 Drug Identification

The identity of cyclosporine was confirmed by high-performance liquid chromatography (HPLC), Fourier transform infrared (FTIR) spectroscopy, differential scanning calorimetry (DSC), and melting point determination.

3.8.1.1 HPLC Analysis

Cyclosporine was analysed using a reverse-phase HPLC system equipped with a Grace Smart™ C18 column (4.6 × 250 mm, 5 µm). The mobile phase consisted of water and acetonitrile (10:90, v/v), delivered at a flow rate of 1.0 mL/min. Detection was carried out at 210 nm, and the column temperature was maintained at 50°C. Standard solutions in the concentration range of 10-100 µg/mL were used for calibration.

3.8.1.2 Fourier Transform Infrared Spectroscopy (FTIR)

FTIR analysis was performed to identify the characteristic functional groups of the pure drug and to evaluate possible interactions between the drug and excipients. Samples were mixed with potassium bromide (KBr), compressed into pellets, and scanned over the range of 4000-400 cm^{-1}.

3.8.1.3 Differential Scanning Calorimetry (DSC)

Thermal characteristics of the drug and formulation components were investigated using DSC. Samples (2-5 mg) were sealed in aluminum pans and heated from 50°C to 170°C at a heating rate of 10°C/min under a nitrogen atmosphere.

3.8.1.4 Melting Point Determination

The melting point of cyclosporine was determined using a digital melting point apparatus to confirm its purity and identity.

3.8.2 Drug-Excipient Compatibility Study

Compatibility between cyclosporine and the selected excipients was evaluated using FTIR spectroscopy by comparing the characteristic absorption peaks of the pure drug and the physical mixtures.

3.8.3 Preparation of Standard Calibration Curve

A standard calibration curve of cyclosporine was developed by HPLC using concentrations ranging from 10 to 100 µg/mL. Peak area was plotted against concentration, and linear regression analysis was performed.

3.8.4 Solubility Study

The solubility of cyclosporine in the selected oil, surfactant, and co-surfactant was determined by the shake-flask method. Excess drug was added to 2 mL of each vehicle and shaken continuously for 24 h at room temperature. After equilibrium, the samples were filtered, suitably diluted, and analyzed by HPLC.

3.8.5 Preparation of Non-Ionic Microemulsion and In-Situ Liquid Crystalline System

3.8.5.1 Construction of Pseudo-Ternary Phase Diagram

Pseudo-ternary phase diagrams were constructed using the water titration method at room temperature. Captex® 300, TPGS, and Span 80 were used as the oil phase, surfactant, and co-surfactant, respectively. The mixtures were gradually titrated with water, and the boundaries of the micro emulsion and liquid crystalline regions were identified based on visual appearance and transmittance.

3.8.5.2 Characterization of Liquid Crystalline System

The phase-transformed system was characterized using various analytical techniques:

Dynamic Light Scattering (DLS): Particle size distribution and changes during water addition were determined using dynamic light scattering.

Differential Scanning Calorimetry (DSC): Thermal transitions associated with liquid crystal formation were evaluated.

Polarized Optical Microscopy (POM): The formation of birefringent liquid crystalline structures was confirmed using a polarized optical microscope.

Cryogenic Scanning Electron Microscopy (Cryo-SEM): The internal morphology and microstructure of the liquid crystalline system were examined.

Rheological Study: The rheological behavior of the formulation at different hydration levels was evaluated using a rotational rheometer.

In-vitro Drug Release Study: Drug release was investigated using the dialysis bag diffusion method. Phosphate buffer (pH 7.4) containing 10% acetonitrile was used as the dissolution medium, and cyclosporine concentration was quantified by HPLC.

3.8.6 Stability Study

The optimized formulation was subjected to short-term stability studies under refrigerated (4°C) and room temperature conditions for 30 days. Samples were evaluated periodically for changes in physical appearance, particle size distribution, and in-vitro drug release characteristics.

4. RESULTS AND DISCUSSION

4.1 Organoleptic Characteristics of Cyclosporine

The organoleptic properties of cyclosporine were evaluated to confirm its physical appearance and purity. The drug was found to be a white, odourless solid, which is in accordance with the reported standard characteristics.

Table 3: Organoleptic characteristics of cyclosporine

Colour	Odour	Appearance
White	Odourless	White solid

4.2 Melting Point Determination

The melting point of cyclosporine was determined by the capillary method using a VEGGO melting point apparatus. The observed melting point was found to be 146°C, which is in close agreement with the reported standard range (148-151°C). The slight variation may be attributed to experimental conditions and indicates the purity and authenticity of the drug sample.

Table 4: Melting point determination of cyclosporine

Standard Value	Observed Value
148-151°C	146°C

4.3 Fourier Transform Infrared (FTIR) Study

4.3.1 FTIR Spectrum of Pure Cyclosporine

The FTIR spectrum of pure cyclosporine exhibited characteristic absorption peaks corresponding to the functional groups present in the molecule. The N-H stretching vibration was observed at 3309.9 cm^{-1}, C-H stretching at 2955.8 cm^{-1}, carbonyl (C=O) stretching at 1617.7 cm^{-1}, and C-N stretching at 1092.1 cm^{-1}. These values were found to be in agreement with reported literature values, confirming the identity of cyclosporine.

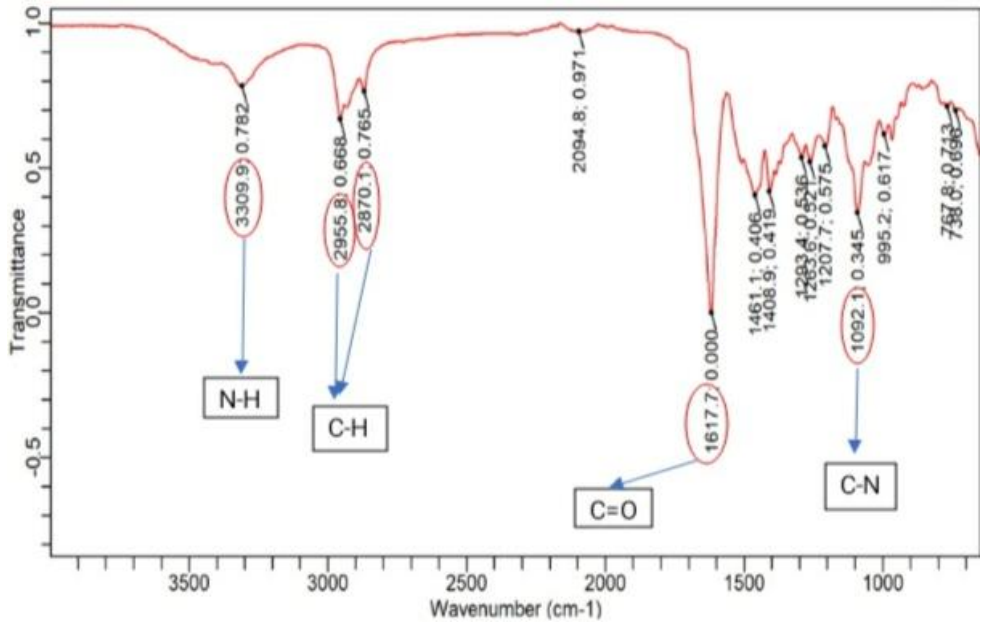

Fig 1: FTIR spectrum of pure cyclosporine

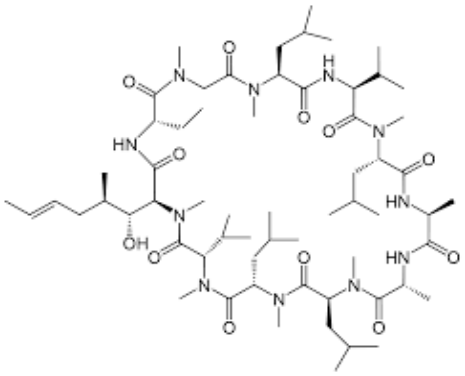

Fig 2: Chemical structure of cyclosporine and FTIR peak interpretation

Table 5: Characteristic FTIR peaks of cyclosporine

Sr. No.	Functional Group	Reported Value (cm^{-1})	Observed Value (cm^{-1})
1	N-H	3200-3600	3309.9
2	C-H	2800-3000	2955.8
3	C=O	1610-1690	1617.7
4	C-N	1266-1342	1092.1

4.3.2 FTIR Spectrum of TPGS Vitamin E

The FTIR spectrum of TPGS showed characteristic peaks of aromatic C-H, carbonyl, C-O, and C-H stretching vibrations, confirming the chemical identity of the selected surfactant.

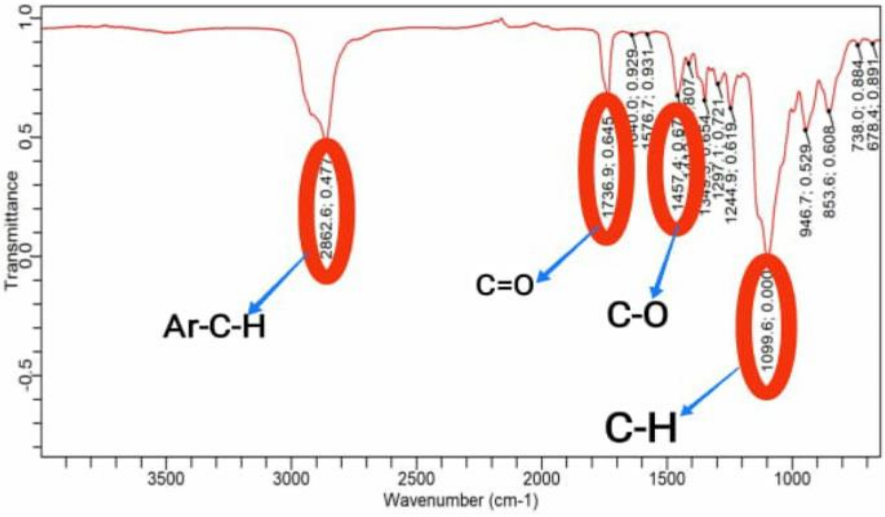

Fig 3: FTIR spectrum of TPGS vitamin E

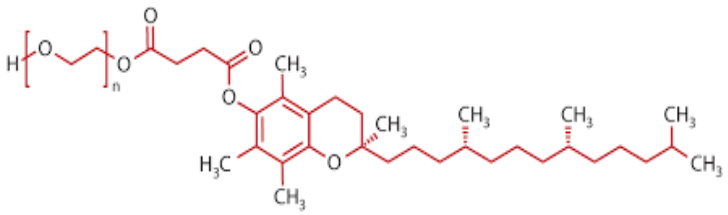

Fig 4: Chemical structure of TPGS vitamin E and FTIR peak interpretation

Table 6: Characteristic FTIR peaks of TPGS vitamin E

Sr. No.	Functional Group	Reported Value (cm^{-1})	Observed Value (cm^{-1})
1	Ar-C-H	2850-3000	2862.6
2	C=O	1610-1690	1736.9
3	C-O	1141-1250	1457.4
4	C-H	2879-2949	1099.6

4.3.3 FTIR Spectrum of Caprylic/Capric Triglyceride

The FTIR spectrum of caprylic/capric triglyceride exhibited characteristic C-H, C=O, and C-O absorption peaks, which were consistent with the standard spectral data reported in the literature.

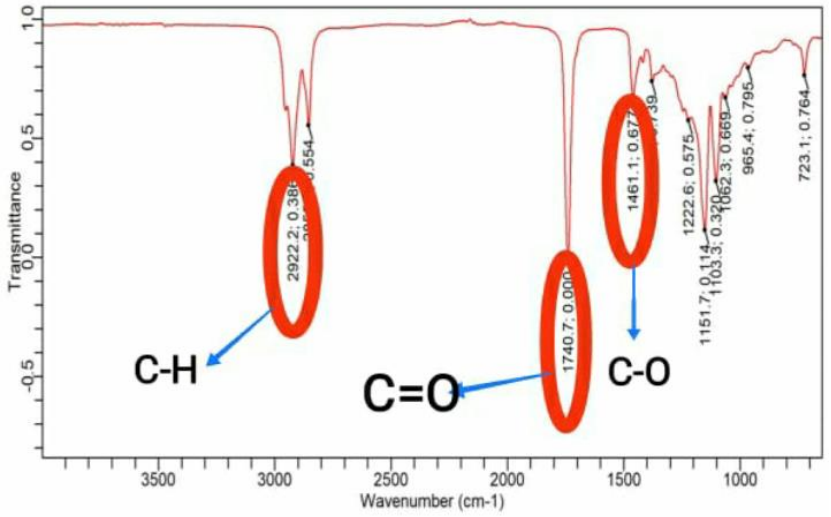

Fig 5: FTIR spectrum of caprylic/capric triglyceride

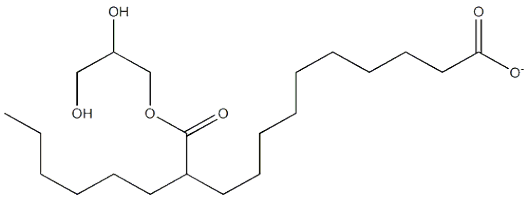

Fig 7: Chemical structure of caprylic/capric triglyceride and FTIR peak interpretation

Table 7: Characteristic FTIR peaks of caprylic/capric triglyceride

Sr. No.	Functional Group	Reported Value (cm^{-1})	Observed Value (cm^{-1})
1	C-H	3000-3100	2922.2
2	C=O	1040-1050	1740.7
3	C-O	1000-1300	1461.1

4.3.4 Drug-Excipient Compatibility Study by FTIR

The FTIR spectrum of the physical mixture containing cyclosporine, TPGS, caprylic/capric triglyceride, and Span 80 retained all the characteristic peaks of the individual components without significant shifting or disappearance. This indicates the absence of any major chemical interaction between the drug and excipients and confirms their compatibility.

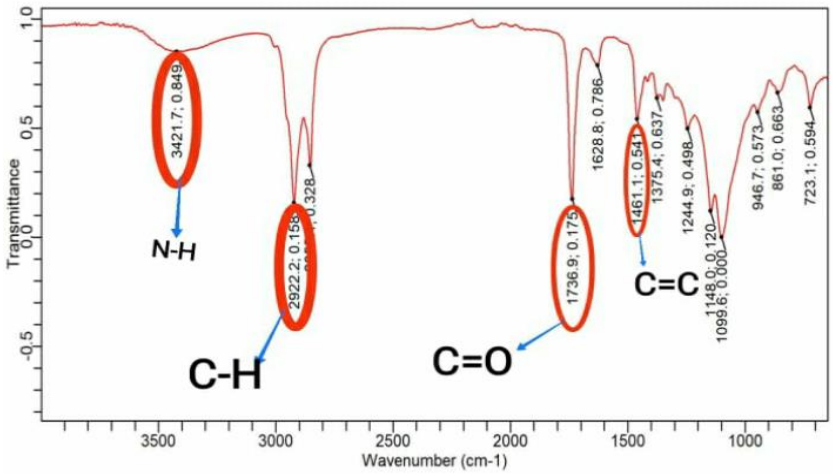

Fig 7: FTIR spectrum of cyclosporine + TPGS + caprylic/capric triglyceride + Span 80

Table 8: Characteristic FTIR peaks of drug-excipient physical mixture

Sr. No.	Functional Group	Reported Value (cm^{-1})	Observed Value (cm^{-1})
1	N-H	3200-3600	3421.7
2	C-H	2800-3000	2922.2
3	C=O	1610-1690	1736.9
4	C=C	1566-1650	1461.1

4.4 HPLC Method Development and Calibration Curve

A reverse-phase HPLC method was developed for the quantitative estimation of cyclosporine. The method showed good linearity over the concentration range of 10-100 µg/mL.

Table 9: Calibration data for cyclosporine

Concentration (µg/mL)	Peak Area
10	20573
20	36341
50	153563

80	230392
100	299620

The calibration plot demonstrated a linear relationship between concentration and peak area, confirming the suitability of the analytical method for quantitative estimation of cyclosporine.

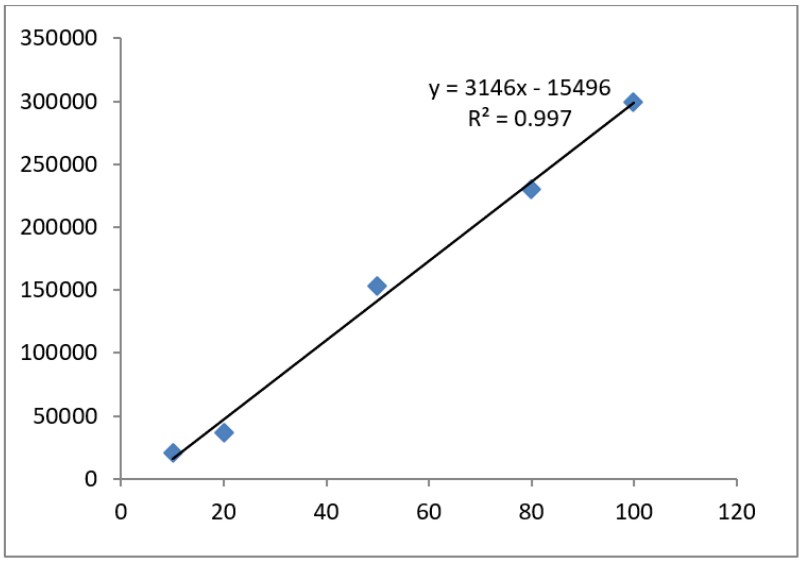

Fig 8: Calibration curve of cyclosporine

The optimized chromatographic conditions were as follows:

- Column: RP-C18
- Mobile phase: Acetonitrile: Water (90:10, v/v)
- Flow rate: 0.65 mL/min
- Detection wavelength: 210 nm
- Retention time: 6.2 min

The chromatogram exhibited a sharp and symmetrical peak with an acceptable retention time, indicating the specificity and reliability of the developed HPLC method.

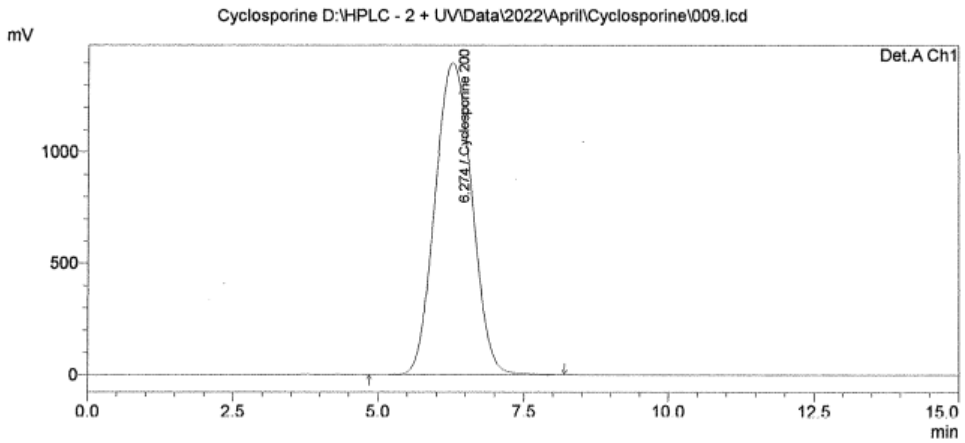

Fig 9: Representative HPLC chromatogram of cyclosporine showing λ_{max} and retention time

4.5 Differential Scanning Calorimetry (DSC) of Cyclosporine

The thermal behavior of pure cyclosporine was evaluated by differential scanning calorimetry (DSC). The thermogram exhibited a distinct endothermic peak at approximately **128.0°C**, which is in close agreement with the reported thermal characteristics of the pure drug. The presence of a sharp melting endotherm confirms the crystalline nature and purity of cyclosporine.

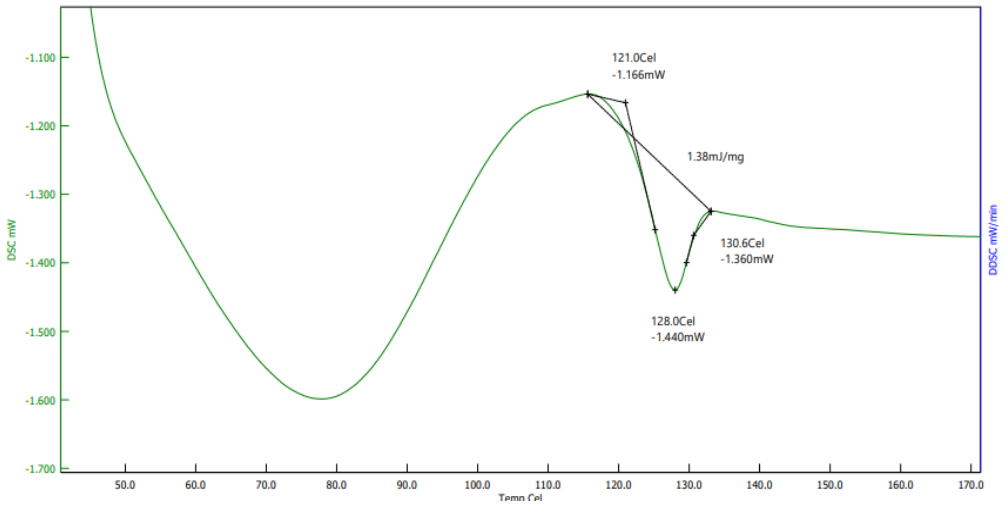

Fig 10: DSC thermogram of pure cyclosporine

4.6 Solubility Study of Cyclosporine

The solubility of cyclosporine was investigated in different formulation components to identify suitable excipients for the development of the non-ionic micro emulsion. Among the tested excipients, cyclosporine showed maximum solubility in **Captex® 300**, followed by **Span 80**, while comparatively lower solubility was observed in **TPGS**.

Table 10: Solubility of cyclosporine in different excipients

Sr. No.	Excipients	Category	Obtained Solubility (mg/mL)	Reported Solubility (mg/mL)
1	Caprylic triglycerides	Oil	96.47 ± 6.15	98.72 ± 7.75
2	TPGS	Surfactant	0.31 ± 0.07	0.29 ± 0.01
3	Span 80	Co-surfactant	19.14 ± 1.16	17.31 ± 1.03

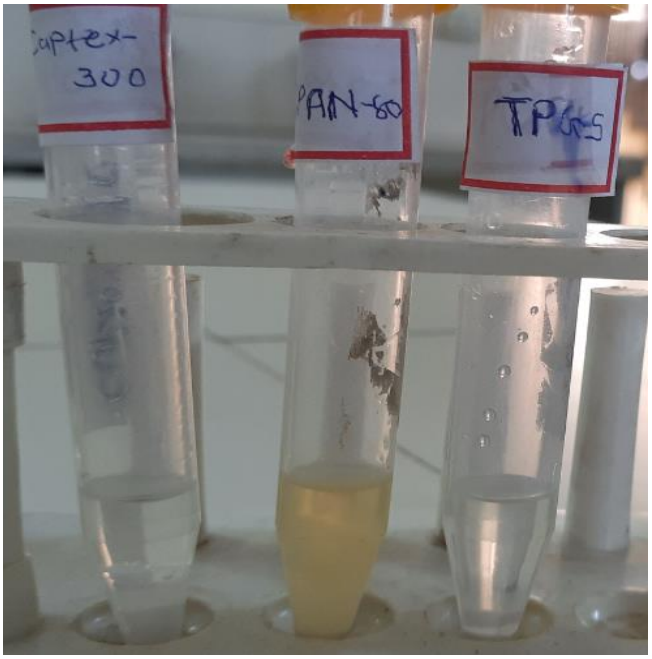

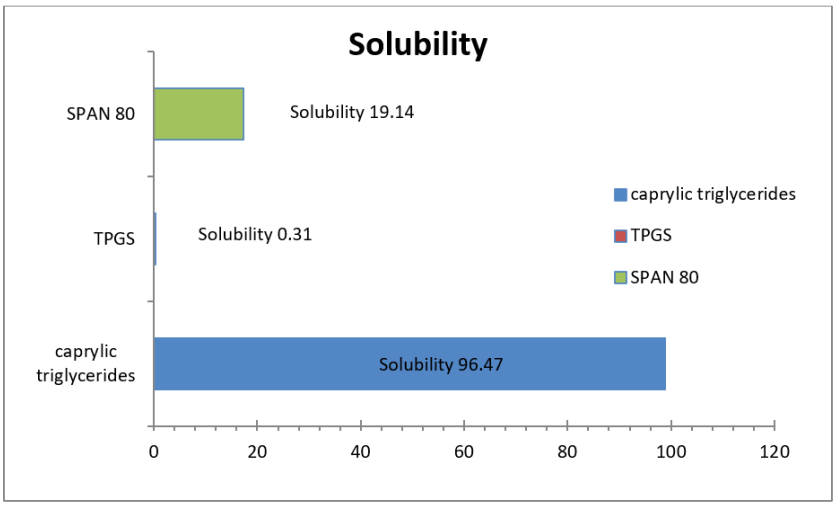

Fig 11: Solubility profile of cyclosporine

Based on the obtained solubility data, Captex® 300 was selected as the oil phase, Span 80 as the co-surfactant, and TPGS as the surfactant for the preparation of the non-ionic micro emulsion.

Table 11: Selection of formulation components

Sr.no	Excipients	Category	Obtained Solubility(mg/ml) n=3(S.D)	Reported Solubility(mg/ml) n=3(S.D)
1	Caprylic triglycerides	Oil	96.47 ± 6.15	98.72 ± 7.75
2	TPGS	Surfactant	0.31 ± 0.07	0.29 ± 0.01
3	SPAN 80	co-surfactant	19.14 ± 1.16	17.31 ± 1.03

4.7 Construction of Pseudo-Ternary Phase Diagram

Pseudo-ternary phase diagrams were constructed to identify the micro emulsion and liquid crystalline regions. The optimized micro emulsion formed spontaneously under gentle magnetic stirring and remained clear and transparent with transmittance values greater than 95%. The average hydrodynamic diameter of the droplets was approximately 26 nm.

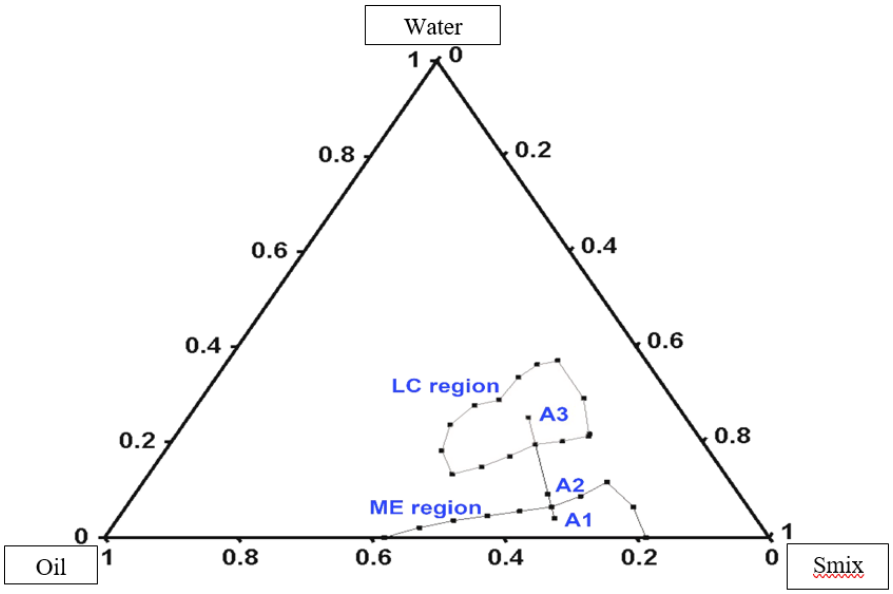

Fig 12: Pseudo-ternary phase diagram showing micro emulsion and liquid crystalline regions

Table 12: Composition of micro emulsion formulations

Formulation	Oil	S-mix	Water
ME1	0.58	0.42	0.000
ME2	0.52	0.46	0.021
ME3	0.46	0.51	0.036
ME4	0.40	0.55	0.045
ME5	0.35	0.60	0.055
ME6	0.30	0.64	0.064
ME7	0.24	0.67	0.087
ME8	0.19	0.70	0.120
ME9	0.17	0.76	0.064
ME10	0.19	0.81	0.000

Table 13: Composition of ME-LC region A

Formulation	Oil	S-mix	Water
ME-LC A1	0.41	0.46	0.13
ME-LC A2	0.36	0.49	0.15
ME-LC A3	0.31	0.52	0.17
ME-LC A4	0.25	0.55	0.19
ME-LC A5	0.21	0.59	0.20
ME-LC A6	0.17	0.62	0.21

Table 14: Composition of ME-LC region B

Formulation	Oil	S-mix	Water

ME-LC B1	0.361	0.40	0.24
ME-LC B2	0.30	0.42	0.28
ME-LC B3	0.26	0.45	0.29
ME-LC B4	0.20	0.45	0.34
ME-LC B5	0.177	0.47	0.36
ME-LC B6	0.13	0.50	0.37

4.8 In-situ Phase Transition upon Water Dilution

The optimized micro emulsion was subjected to progressive water addition along the selected dilution line. Gradual hydration resulted in transformation from a clear isotropic micro emulsion to a highly viscous liquid crystalline system.

Formulation A1 remained transparent with approximately 6.4% water incorporation, while A2 and A3 demonstrated increasing viscosity and phase transition due to additional water uptake.

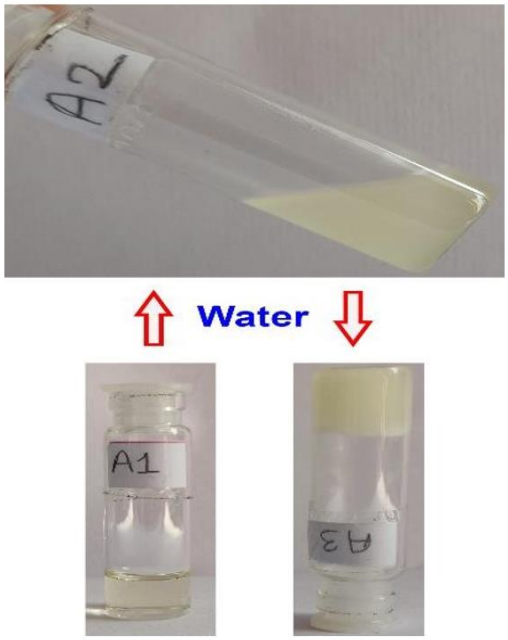

Fig 13: Visual phase transition of micro emulsion during water addition

Table 15: Composition of formulations used for phase transition study

Formulation	Oil	S-mix	Water
A1	0.30	0.66	0.040
A2	0.29	0.62	0.090
A3	0.24	0.51	0.252

The successful in-situ transformation into a liquid crystalline phase suggests that the developed formulation can serve as a stable depot system for the prolonged and controlled release of cyclosporine.

4.9 Rheological Study

The rheological behavior of the optimized formulations was investigated to evaluate the effect of water-induced phase transformation on viscosity. The viscosity of formulations B1, B2, and B3 was measured at a constant shear rate of 10 s^{-1}. A significant increase in viscosity was observed with increasing water content, indicating the gradual formation of a structured liquid crystalline network. The enhanced viscosity is expected to contribute to prolonged drug retention and sustained drug release.

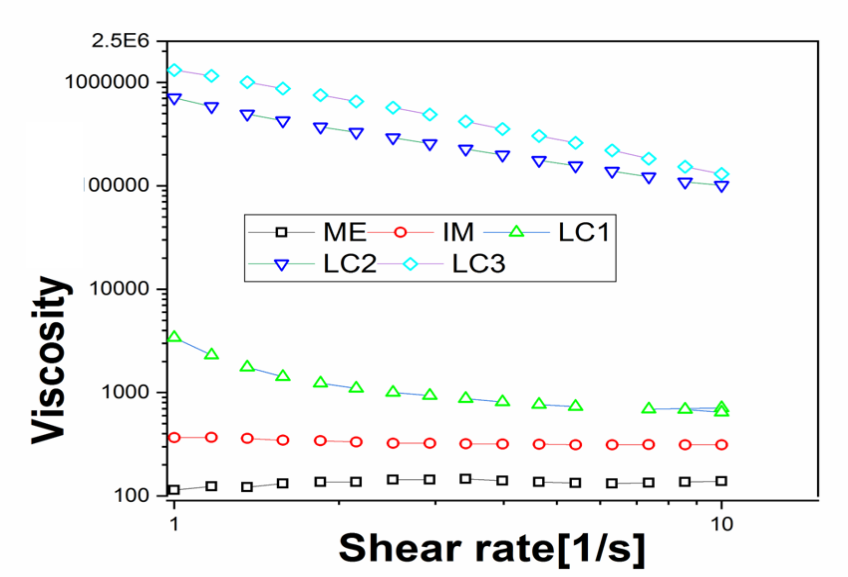

Fig 14: Viscosity of micro emulsion and liquid crystalline formulations

4.10 Effect of Water Addition on Droplet Size Distribution

Dynamic light scattering (DLS) was employed to investigate the changes in droplet size during the hydration process. The optimized micro emulsion composition (oil/water/Smix = 0.296/0.064/0.64) was selected for the study because it was located near the phase boundary.

A substantial increase in droplet size was observed with progressive water addition. The appearance of larger aggregates and increased polydispersity indicated the onset of phase transformation. At higher water levels, the formulation became highly viscous and eventually transformed into a stiff gel-like liquid crystalline system.

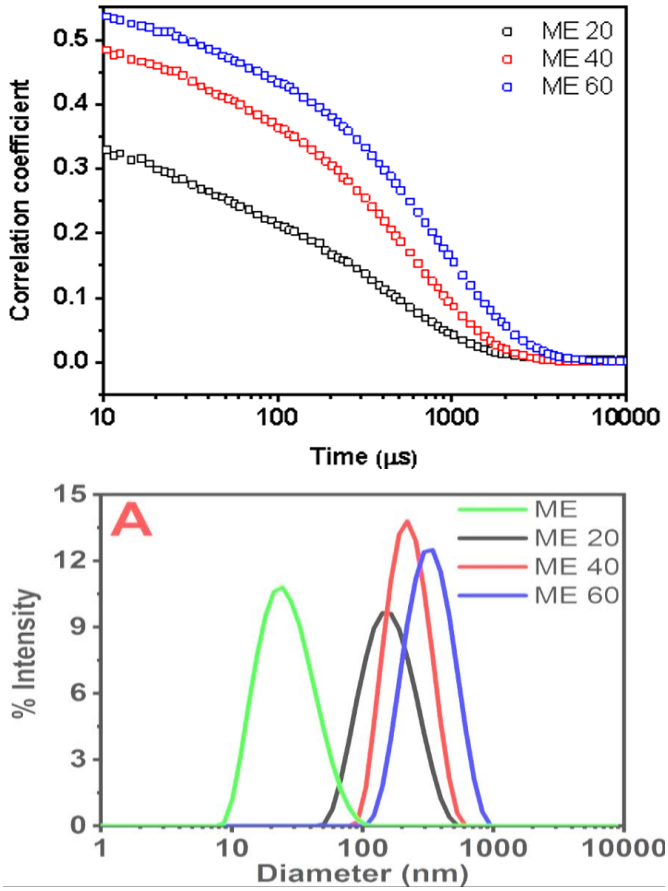

Fig 15: Changes in droplet size distribution during water addition

Cryo-SEM analysis further confirmed the structural transformation. The images revealed that the initially spherical droplets became interconnected through aqueous channels, indicating the formation of a highly organized liquid crystalline network.

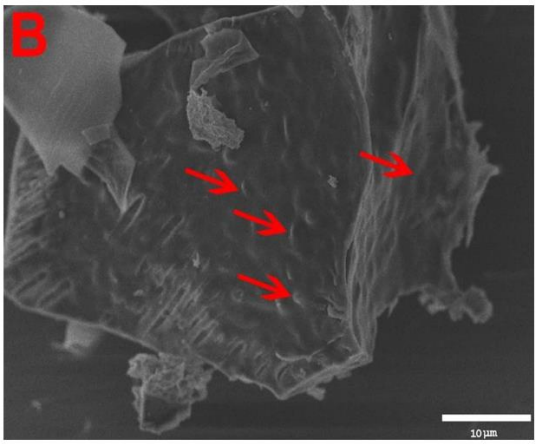

Fig 16: Cryo-SEM image of the liquid crystalline structure

The phase transformation remained unaffected after sterilization and freeze-thaw cycles, demonstrating the robustness of the developed formulation.

4.11 Polarized Light Microscopy Study

The water-induced phase transition was further confirmed by polarized light microscopy. Initially, the micro emulsion appeared isotropic without birefringence. As water content increased, birefringent domains characteristic of liquid crystalline structures became visible.

At higher hydration levels, the birefringence intensified and occupied the entire microscopic field, confirming the formation of a stable liquid crystalline phase. Similar observations were obtained for the cyclosporine-loaded formulation, indicating that drug incorporation did not interfere with phase transformation.

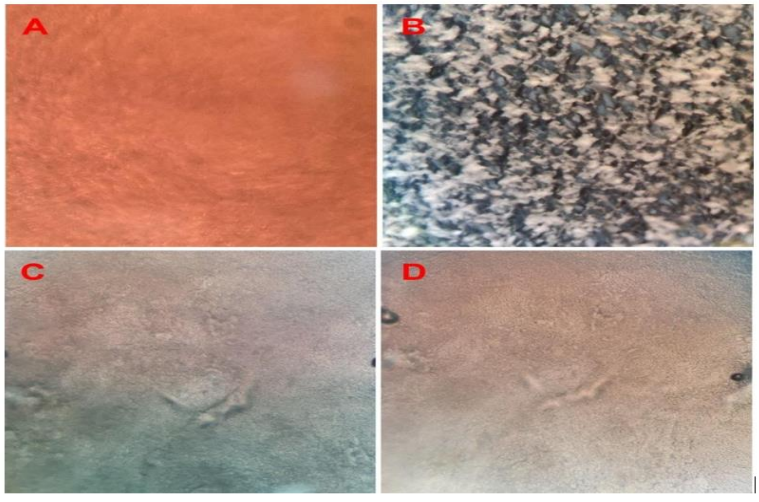

Fig 17: Polarized microscopic images showing transition from micro emulsion to liquid crystalline phase

To further visualize the interfacial phenomenon, one drop of micro emulsion and one drop of water were brought into contact on a microscope slide. A thick birefringent liquid crystalline layer was formed immediately at the interface, restricting further diffusion of water into the formulation.

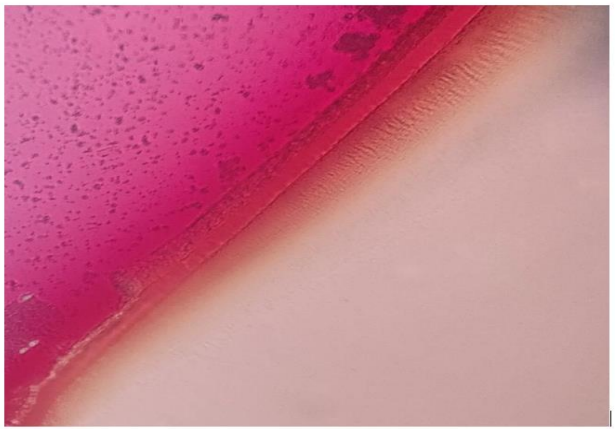

Fig 18: Microscopic observation of the micro emulsion-water interface showing birefringence

The formation of this highly viscous liquid crystalline shell may act as a diffusion barrier and contribute to the controlled release behavior of the developed formulation.

4.12 Differential Scanning Calorimetry of Microemulsion and Liquid Crystalline System

DSC analysis was carried out to investigate the thermal events associated with the hydration-induced phase transition. The thermograms of the blank formulation exhibited characteristic crystallization and melting transitions, confirming the structural rearrangement occurring during liquid crystal formation.

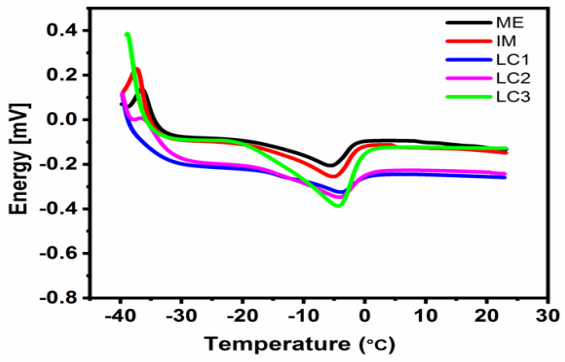

Fig 19: DSC thermograms of blank micro emulsion during water addition

With increasing water content, the melting endotherms became broader and more distinct, suggesting stable incorporation of water molecules within the hydrated surfactant matrix.

The DSC thermograms of the cyclosporine-loaded formulation showed a single melting transition without the appearance of additional crystalline peaks. The absence of a separate drug melting endotherm suggests that cyclosporine remained molecularly dispersed within the liquid crystalline matrix.

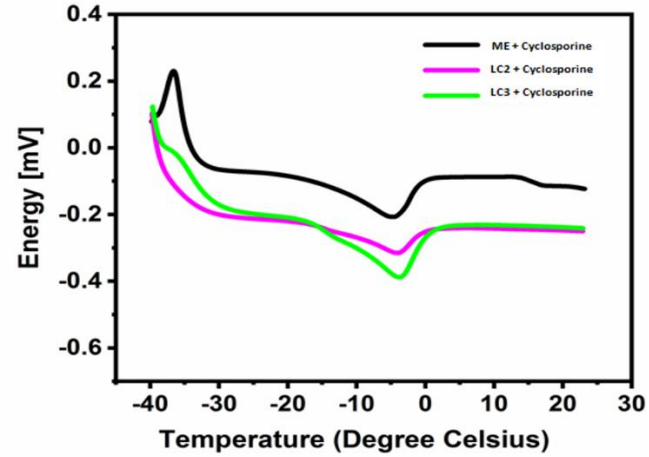

Fig 20: DSC thermograms of cyclosporine-loaded micro emulsion during water addition

4.13 In-vitro Drug Release Study

The in-vitro release profile of cyclosporine from the optimized formulation was compared with that of the pure drug suspension.

Table 16: Comparative in-vitro drug release profile

Sr. No.	Time (h)	% Cumulative Drug Release (Pure Drug)	% Cumulative Drug Release (Optimized Formulation)
1	0.5	12.00	6.48
2	1	25.00	17.87
3	1.5	47.00	22.77
4	2	69.00	27.49
5	3	82.00	36.66
6	4	96.00	44.48
7	8	-	67.61
8	12	-	79.93
9	24	-	89.24

The optimized micro emulsion exhibited a sustained release pattern compared with the pure drug. The formation of an in-situ liquid crystalline depot effectively retarded drug diffusion and prolonged the release of cyclosporine over 24 hours.

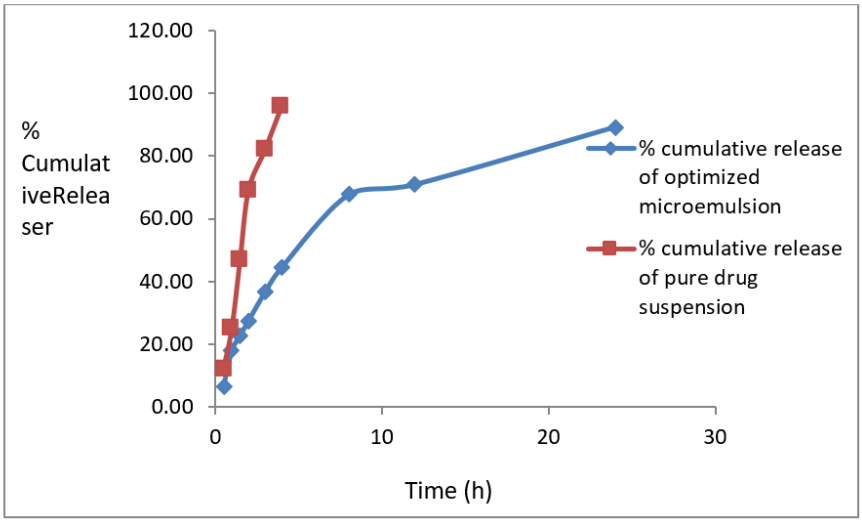

Fig 21: Comparative in-vitro drug release profile of pure drug and optimized formulation

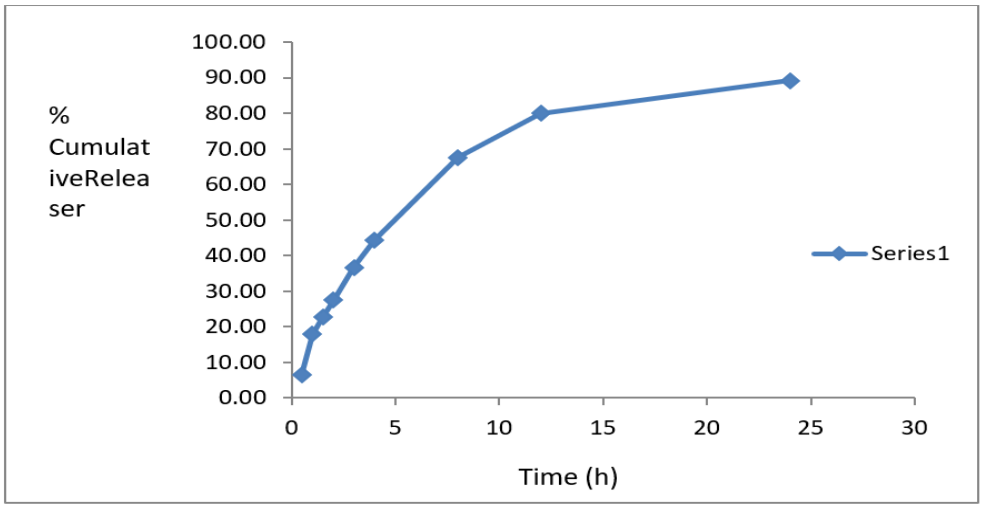

Fig 22: Plot of cumulative drug release versus time

The integrity of the liquid crystalline matrix was maintained throughout the release study, and no evidence of phase inversion was observed.

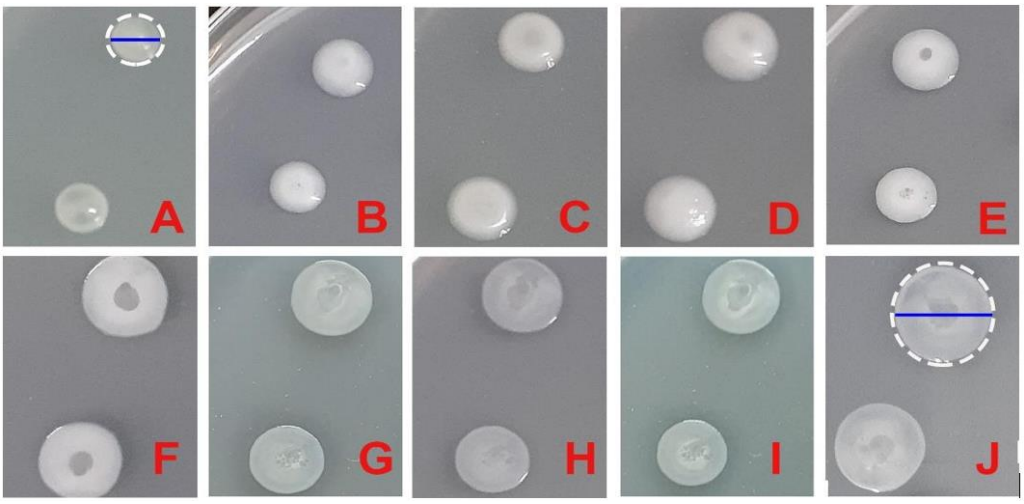

Fig 23: Time-dependent changes in the liquid crystalline formulation on agar surface

4.14 Stability Study

The optimized formulation was subjected to short-term stability studies under refrigerated conditions (4°C) for one month. No visible phase separation, drug precipitation, or significant change in appearance was observed during the storage period.

The cumulative drug release after one month was found to be 88.37%, which was comparable to the initial value, indicating good formulation stability.

Table 17: Accelerated stability study of optimized formulation

Time (h)	Initial (% CDR)	After 1 Month (% CDR)
0.5	6.48	6.38
1	17.87	16.54
1.5	22.77	22.65
2	27.49	26.29
3	36.66	34.98
4	44.48	44.27
8	67.61	65.84
12	79.93	69.89

24	89.24	88.37

The stability results demonstrate that the developed non-ionic micro emulsion maintained its physicochemical properties and controlled drug release characteristics during storage.

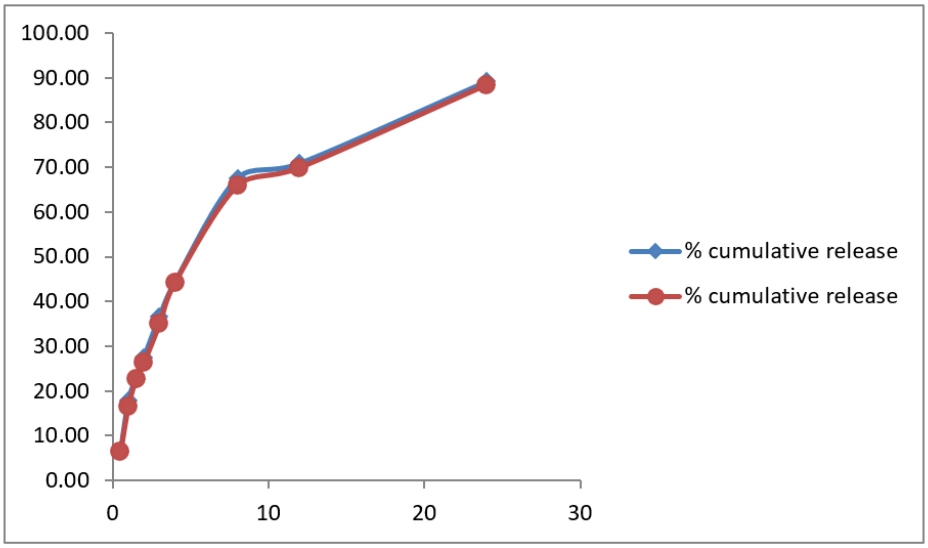

Fig 24: Accelerated stability study

Conclusion

This study demonstrates water-driven transformation of a nonionic ME into rigid LC phase. The formulation was composed of TPGS-Span 80 (3:1) and Captex 355, respectively, as surfactant mixture and oil phase. Phase boundary corresponding to isotropic ME and birefringent LC structure was delineated in the pseudoternary phase diagram. The transition was studied at the level of surfactants and during water incorporation in complete oil phase. Water incorporation into oil phase triggered progressive conversion of isotropic ME into birefringent LC phase with superior physical properties. It remained stable at physiological temperature until 72 h and offered controlled released of cyclosporine under artificial sink conditions. We speculate that fluidity of ME would enable its convenient intra-muscular placement whereupon it can undergo transition to form a controlled release depot. Coupled with enhanced cyclosporine solubilization, the approach can be valuable for minimizing the post-surgical recurrence arising from the micro- deposits of tumor cells.

LIST OF ABBREVIATIONS

FT-IR	Fourier Transform Infrared
DSC	Differential scanning colorimetry
ICH	International Conference on Harmonization
HPLC	High Performance Liquid Chromatography
SEM	Scanning electron microscopy
% CDR	Cumulative drug release
PDI	Polydispersity index
RT	Room temperature

1. Shaikh MI, Raval AM, Development and Validation of RP-HPLC Method for Simultaneous Estimation of Metformin Hydrochloride, Linagliptin and Dapagliflozin in Synthetic Mixture, Asian Journal of Pharmaceutical Research and Development. 2026; 14(3):18-30, DOI: http://dx.doi.org/10.22270/ajprd.v14i3.1767
2. Goswami V, Shukla R, Patel B, Suthar A, Patel P, Raval AM. HPTLC Method Development and Validation for Simultaneous Estimation of Rifaximin and Metronidazole Benzoate in Combined Tablet Dosage Form. Int J Drug Deliv Technol. 2026; 16(46s): 257-265. DOI: 10.25258/ijddt.16.46s.27
3. Joshi SY, Detholia KK, Raval AM, Dharu NR, Rathod SR, Kushkiwala AM. Development and Validation of a Stability-Indicating RP-HPLC Method for Quantitative Estimation of Sunitinib Malate in Pharmaceutical Dosage Form. Int J Drug Deliv Technol. 2026; 16(12s): 418-426. DOI: 10.25258/ijddt.16.12s.48
4. PatelK, BharatiyaB, KadamY, "Micellization and clouding behavior of EO–PO block copolymer in aqueous salt solutions."Journal of Surfactants Detergents.2010, 13:89-95.
5. GeethuP, YadavI, AswalVK, "Enhancement in Elastic Bending Rigidity of Polymer Loaded Reverse Microemulsions." Langmuir. 2017, 33:13014-26.
6. Tiwari S, Tirosh B, Rubinstein A. "Increasing the affinity of cationized polyacrylamide-paclitaxel nanoparticles towards colon cancer cells by a surface recognition peptide."International Journal of Pharmaceutics. 2017, 531:281-91.
7. ChatOA, NazirN, "Aggregation and Rheological Behavior of the Lavender Oil-Pluronic P123 Microemulsions in Water-Ethanol Mixed Solvents." Langmuir.2018, 34:1010-9.
8. F. Reinitzer, "Contributions to the knowledge of cholesterol."Monatsh. Chem., 1888, 9, 421-441.
9. O. Lehmann, "Liquid Crystals arrive back home at their birthplace" z.Physik. Chem., 1889, 4, 462.
10. G. Petrov, The lyotropic state of matter: molecular physics and living matter physics." Gorden and Breach Science. 1999.
11. Friedel G, "Universe and Matter Conjectured as a 3-Dimensional Lattice with Topological Singularities" Ann. Physiqu., 1922, 18, 273.
12. Collings P.J. and Hird M., In Introduction to Liquid Crystals Chemistry and Physics; 1st Edn; Taylor and Francis Ltd, UK, 2004.pp 314.
13. Goodby J.W., "Handbook of Liquid crystals." Weinheim, 1998.
14. Helfrich W., "Electric -ol. Cryst. Liq. Cryst., 1973, 21, 187.
15. Schadt M., "liquid crystal materials and liquid crystal displays."Ann. Rev. Mater. Sci., 1997, 27, 305.
16. Meier G., Sackmann E. and Grabmaier J.G., "Application of liquid crystals." Springer Verlag, 1975.
17. Takatoh K., Hasegawa M., "Alignment Technologies and Applications of Liquid Crystal Devices." Taylor and Francis Ltd., New York, USA, 2005.
18. Yang D. K. and Wu S. T., "Fundamentals of Liquid Crystal Devices." John Wiley & Sons Ltd., Chichester, UK, 2006.
19. GoemaereS, Ackerman C, Goethals K, "Onset of symptoms of rheumatoid arthritis in relation to age, sex and menopausal transition."J Rheumatol. 1990, 17, 1620-1622.
20. Sangha O, "Epidemiology of rheumatic diseases." Rheumatology 39, 2000 3-12.
21. Garrod A, "A Treatise on Gout and Rheumatic Gout." London, Longman Green, 1876.
22. Rothschild BM, Turner KR, DeLuca MA, "Symmetrical erosive peripheral polyarthritis in the late archaic period of Alabama." Science 241, 1988, 1498.
23. Spector TD, Hochberg MC, "The protective effect of the oral contraceptive pill on rheumatoid arthritis: an overview of the analytic epidemiological studies using meta analysis." J Clin Epidemiol 43, 1990, 1221.

24. Peschken CA, El-gabalawy HS, Roos LL, “Algonkian Indians have twice the frequency of rheumatoid arthritis with a younger age of onset.” Arthritis Rheum 41(suppl.9), 1998, Abstract #558.
25. Mitchell DM, “Epidemiology, rheumatoid arthritis, etiology, diagnosis and treatment.” Philadelphia, PA: JB LippincottCo., 1985.
26. Mevada J, Patel K, Raval AM. Materiovigilance: From device failure to safety reform, the growing importance of materiovigilance systems. Int J Pharm Sci. 2026; 4(1):962-74.
27. Falwariya, R., Jethva, T., Raval, A.M. and Lokhande, D., 2026. Comprehensive review: Microneedle patches-A painless revolution in transdermal drug delivery. World J Pharm Med Res, 12(1), pp.199-207.
28. Mevada J, Patel K, Raval AM. Role of pharmacovigilance in drug safety monitoring. World J Pharm Med Res. 2025; 11(11):235-40.
29. Rathi S. Physicochemical Characterization and In-Vitro Dissolution Enhancement of Ranolazine Using Solid Dispersion Method. Available at SSRN 3507970. 2019 Dec 21.
30. Raval AM, Bhavsar PR, Pandya FU, Patel D. Co-processed excipients in pharmaceutical formulation: advances, characterization, and applications. Asian Journal of Pharmaceutical Research and Development. 2026 Feb 16; 14(01):105-13.
31. Patel N, Raval AM. Gastro-retentive drug delivery system: A review. Int J Pharm Sci. 2026;4(1):734-42.
32. Zankhwala MF, Raval MA, Kushkiwala MA, Sarvaiya MS, Raval MK, Thakar MN, Barjod MS. Formulation And Evaluation Of Optimized Polymer Blends For Diclofenac Diethylamine Transdermal System. The Review of Diabetic Studies. 2025 Sep 14:701-8.
33. Kushkiwala AM, Zankhwala FM, Patel MD, Raval AM. Flurbiprofen loaded ethosomal gel: Design, optimization, and anti-inflammatory activity. Int J Res Anal Rev. 2024; 11(4):709-42.
34. Raval MA, Suthar MA, Durani MB, Thakar MN, Zankhwala MF, Kushkiwala MA, Rathod MS. Smart Co-Processed Excipient Platforms: A Novel Strategy for Multifunctional Optimization of Ibuprofen Tablet Formulations. practice; 1:2.
35. Golwala P, Rathod S, Patil R, “Effect of cosurfactant addition on phase behavior and microstructure of a water dilutable microemulsion.” Colloids and Surfaces B: Biointerfaces, 2020, 186:110736.